Correlation of CrOCr π-Bonding Strength with π-Donor Effectiveness of Bridging and Nonbridging Ligands in (Tris(2-pyridylmethyl)amine)chromium(III) Dimers

Thomas F. Tekut,[†] Charles J. O'Connor,[‡] and Robert A. Holwerda*,[†]

Department of Chemistry and Biochemistry, Texas Tech University, Lubbock, Texas 79409, and Department of Chemistry, University of New Orleans, New Orleans, Louisiana 70148

Received June 1, 1992

The preparations of two $[Cr(tmpa)L]_2O^{2+}$ dimers in which the pseudohalide ligand is a weaker π-donor than NCS^- are reported (tmpa = tris(2-pyridylmethyl)amine): $[Cr(tmpa)(NCSe)]_2O(ClO_4)_2$ and $[\{Cr(tmpa)(NCS)\}_2(O)Pd(CA)](ClO_4)_2 \cdot 2CH_3CN$; CA^{2-} = 2,5-dioxo-3,6-dichloro-1,4-benzoquinone. The NCS^- ligands are constrained to lie on the same side of the CrOCr bond axis by chelation of the Pd(II) center in the latter complex, contrary to the anti orientation of the parent dimer. $[Cr(tmpa)(NCSe)]_2OH^{3+}$ (pK_a = 1.48) and $[\{Cr(tmpa)(NCS)\}_2(OH)Pd(CA)]^{3+}$ (pK_a = 1.15) are more acidic than $[Cr(tmpa)(NCS)]_2OH^{3+}$ by factors of 3.7 and 7.9, respectively. ^1H NMR spectra demonstrate that all $[Cr(tmpa)L]_2O^{2+}$ complexes reported to date have symmetric chelation by the tmpa ligands in which both apical N atoms are cis to the oxo bridge. A linear correlation of Cr(III,IV/III,III) half-wave reduction potential with $pK_a(Cr(\mu\text{-}OH)Cr)$ pertains for both singly- and doubly-bridged (tmpa)CrOCr(tmpa) dimers, with the exception of $[Cr(tmpa)(CN)]_2O^{2+}$. On this basis, it is concluded that the b_{2g} HOMO energy increases with π-donor effectiveness of both bridging and nonbridging ligands, in the following order: $\mu\text{-}C_6H_5CO_2^- \approx \mu\text{-}HCO_2^- < \mu\text{-}CH_3CO_2^- \approx NCS^- < NCO^- \approx Cl^- < N_3^- \ll \mu\text{-}F^- < \mu\text{-}OH^-$. The trend toward larger pK_a of $Cr(\mu\text{-}OH)Cr$ conjugate acids with increasing substituent π Lewis basicity shows that CrOCr π-bonding strength is highly sensitive to the competition between $\mu\text{-}O^{2-}$ and $\mu\text{-}X^-$ or L^- groups for donation to the metal. In this way, both the reduced oxo group basicities and the diamagnetism of the $NCSe^-$ and $NCS\{Pd(CA)/2\}^-$ derivatives may be understood.

Introduction

The structural, spectroscopic, magnetic, and electrochemical properties of linear, oxo-bridged transition metal dimers are generally consistent with the Dunitz–Orgel model of bridge-bonding.[1-4] Thus, all three reported crystal structures of $\mu\text{-}O^{2-}$ chromium(III) dimers[5-7] feature a Cr–O–Cr bond angle at or near the value of 180° expected for maximal $Cr(d\pi)\text{–}O(p\pi)$ overlap and Cr–O bond lengths (1.80–1.82 Å) consistent with partial double bond character. Oxo-bridged chromium(III) dimers with diimine and pseudohalide ligands[8] exhibit diamagnetic ground states and weaker $\mu\text{-}O^{2-}$ group basicity as compared with the linear, centrosymmetric $[Cr(tmpa)(NCS)]_2O^{2+}$ complex; tmpa = tris(2-pyridylmethyl)amine. Although $[Cr(tmpa)(NCS)]_2O^{2+}$ undergoes one-electron oxidation ($E_{1/2}$ = 1.17 V vs NHE in CH_3CN, 0.1 M $N(n\text{-}Bu)_4ClO_4$, 25 °C)[7] to give a relatively stable mixed-valence Cr(III,IV) species,[3] analogous oxidation products of $[Cr(bpy)_2(NCS)]_2O^{2+}$ and $[Cr(phen)_2(NCS)]_2O^{2+}$ decay rapidly through internal electron transfer from the NCS^- ligands, implicating strong conjugation of the highest occupied molecular orbital with both π-accepting diimine and π-donating pseudohalide substituents.[8]

The D_{4h} π-electronic configuration $(e_u^b)^4(e_g)^4(b_{2g})^2(b_{1u})^0$ accounts well for the magnetic, spectroscopic and electrochemical characteristics of CrOCr dimers with aromatic amine and diimine ligands; the b_{2g} HOMO level has the correct symmetry to interact with pyridyl π^* orbitals and $p\pi$-donor orbitals of halide and pseudohalide ligands, while the b_{1u} LUMO is nonbonding in the absence of Cr–Cr δ interaction.[3,8] To complete our investigations of substituent effects in $[Cr(tmpa)L]_2O^{2+}$ complexes, we report here two dimers in which the pseudohalide ligand is a weaker π-donor than NCS^-, $[Cr(tmpa)(NCSe)]_2O^{2+}$ and $[\{Cr(tmpa)(NCS)\}_2(O)Pd(CA)]^{2+}$; CA^{2-} = 2,5-dioxo-3,6-dichloro-1,4-benzoquinone. Thus, the N=C=Se resonance form contributes less to the bonding in $NCSe^-$ than does N=C=S to the electronic structure of NCS^-.[9] In the palladium derivative, NCS^- to Cr(III) π-donation is attenuated by the electrophilic, S-bonded Pd(II) substituent, and the NCS^- ligands are constrained to lie on the same side of the CrOCr bond axis, contrary to the anti orientation documented for the parent dimer.[7]

Experimental Section

Materials and Methods. Reagent grade chemicals and distilled solvents were used throughout. $[Pd(CA)(CH_3CN)_2]$, $[Cr(tmpa)(OH)]_2(ClO_4)_4 \cdot 4H_2O$, $[(tmpa)Cr(O)(F)Cr(tmpa)](ClO_4)_3 \cdot H_2O$, $[Cr(bpy)_2(NCS)]_2OH(ClO_4)_3 \cdot 2H_2O$, $[Cr(tmpa)(NCS)_2](ClO_4)$, $[H_3tmpa](ClO_4)_3$, and dimers of the form $[Cr(tmpa)L]_2O(ClO_4)_2$ (L^- = Cl^-, NCS^-, NCO^-, CN^- and N_3^-) were available from laboratory stock.[3,10-12] $[PdCl_2(CH_3CN)_2]$ and KNCSe were purchased from Aldrich. UV–vis and IR (KBr pellet) spectra were acquired on Shimadzu UV-260 and Perkin-Elmer Model 1600 instruments, respectively. Spectrophotometric titrations, cyclic voltammetric scans, and magnetic susceptibility measurements (4–300 K) were carried out and quantitatively interpreted as previously described.[3] ^1H NMR spectra were recorded on a Bruker 200-MHz spectrometer; chemical shifts are reported in parts per million (δ) downfield from TMS.

Synthesis of $[Cr(tmpa)(NCSe)]_2O(ClO_4)_2$. $[Cr(tmpa)(OH)]_2(ClO_4)_4 \cdot 4H_2O$ (1.00 g, 0.841 mmol) was dissolved in 100 mL of CH_3CN and mixed with a 10-fold excess of KNCSe (1.2121 g, 8.41 mmol) at room temperature, affording an immediate purple precipitate of [Cr(tmpa)-

[†] Texas Tech University.
[‡] University of New Orleans.

(1) Dunitz, J. D.; Orgel, L. E. *J. Chem. Soc.* **1953**, 2594.
(2) Holm, R. H. *Chem. Rev.* **1987**, *87*, 1401.
(3) Gafford, B. G.; O'Rear, C.; Zhang, J. H.; O'Connor, C. J.; Holwerda, R. A. *Inorg. Chem.* **1989**, *28*, 1720.
(4) Cotton, F. A.; Najjar, R. C. *Inorg. Chem.* **1981**, *20*, 1866.
(5) Yevitz, M.; Stanko, J. A. *J. Am. Chem. Soc.* **1971**, *93*, 1512.
(6) DiVaira, M.; Mani, F. *Inorg. Chem.* **1984**, *23*, 409.
(7) Gafford, B. G.; Holwerda, R. A.; Schugar, H. J.; Potenza, J. A. *Inorg. Chem.* **1988**, *27*, 1126.
(8) Holwerda, R. A.; Tekut, T. F.; Gafford, B. G.; Zhang, J. H.; O'Connor, C. J. *J. Chem. Soc., Dalton Trans.* **1991**, 1051.
(9) *Chemistry of the Pseudohalides*; Golub, A. M., Kohler, H., Skopenko, V. V., Eds.; Elsevier: New York, 1986.
(10) Gafford, B. G.; Holwerda, R. A. *Inorg. Chem.* **1989**, *28*, 60.
(11) Gafford, B. G.; Holwerda, R. A. *Inorg. Chem.* **1990**, *29*, 4353.
(12) Jeong, W.-Y.; Holwerda, R. A. *Inorg. Chem.* **1988**, *27*, 2571.

0020-1669/93/1332-0324$04.00/0

$(OH)]_2(NCSe)_4$. Overnight stirring of the reaction mixture at 70 °C converted this precursor to insoluble, green $[Cr(tmpa)(NCSe)]_2O(NCSe)_2$, which was filtered off and washed with ether. This intermediate was dissolved in the minimum volume of *N,N*-dimethylformamide and added dropwise to aqueous 0.1 M $LiClO_4$, yielding a precipitate of $[Cr(tmpa)(NCSe)]_2O(ClO_4)_2$. The product was washed with water and ether and vacuum-dried. Yield: 0.69 g, 74%. Anal. Calcd for $[Cr(tmpa)(NCSe)]_2O(ClO_4)_2$: Cr, 9.37; C, 41.13; H, 3.27; N, 12.62. Found: Cr, 9.14; C, 40.97; H, 3.22; N, 12.25. IR: ν_{as}(CrOCr) = 832, 843, 855 cm^{-1}; ν(C≡N) = 2047 cm^{-1}. UV–vis (CH_3CN; λ_{max}, nm (ϵ, M^{-1} cm^{-1})): 357 (1.73×10^4), 416 (2.60×10^3).

Preparations of $[\{Cr(tmpa)(NCS)\}_2(O)Pd(CA)](ClO_4)_2 \cdot 2CH_3CN$ and $[Cr(tmpa)(NCS)_2Pd(CA)](ClO_4) \cdot 2CH_3CN$. $[Cr(tmpa)(NCS)]_2O(ClO_4)_2 \cdot H_2O$ (0.100 g, 0.0967 mmol) was dissolved in 50 mL of CH_3CN and mixed with $[Pd(CA)(CH_3CN)_2]$ (0.0383 g, 0.0967 mmol) at room temperature. The brown precipitate which developed within 30 min was filtered off, washed with ether, and vacuum-dried. Yield: 96 mg, 70%. Decomposition of the Pd(CA) adduct was noted upon prolonged standing of the supernatant at room temperature. Anal. Calcd for $[\{Cr(tmpa)(NCS)\}_2(O)Pd(C_6O_4Cl_2)](ClO_4)_2 \cdot 2CH_3CN$: C, 40.85; H, 3.00; N, 11.91. Found: C, 41.21; H, 3.12; N, 11.83. IR: ν_{as}(CrOCr) = 845 cm^{-1}; ν(C≡N) = 2049 s, 2106 w, 2151 w cm^{-1}; ν(C—Cl) = 858 cm^{-1}; ν(C=O) = 1655, 1676, 1701 cm^{-1}. UV–vis (CH_3CN; λ_{max}, nm (ϵ, M^{-1} cm^{-1})): 257 (3.7×10^4), 303 (2.9×10^4). $[Cr(tmpa)(NCS)_2Pd(CA)](ClO_4) \cdot 2CH_3CN$ was prepared similarly from the reaction between equimolar quantities of $[Cr(tmpa)(NCS)_2](ClO_4)$ and $[Pd(CA)(CH_3CN)_2]$. Anal. Calcd for $[Cr(tmpa)(NCS)_2Pd(C_6O_4Cl_2)](ClO_4) \cdot 2CH_3CN$: C, 37.79; H, 2.54; N, 11.75. Found: C, 37.97; H, 2.21; N, 11.34. IR: ν(C≡N) = 2035 s, 2107 w, 2142 w cm^{-1}; ν(C—Cl) = 858 cm^{-1}; ν(C=O) = 1654, 1676, 1702 cm^{-1}. UV–vis (CH_3CN; λ_{max}, nm (ϵ, M^{-1} cm^{-1})): 263 (2.2×10^4), 299 (2.2×10^4), 342 sh (1.3×10^4).

Reactions of $[Cr(tmpa)(NCS)]_2O(ClO_4)_2$ with $[PdCl_2(CH_3CN)_2]$ and $AgNO_3$. $[PdCl_2(CH_3CN)_2]$ (0.0251 g, 0.0967 mmol) was mixed with $[Cr(tmpa)(NCS)]_2O(ClO_4)_2 \cdot H_2O$ (0.100 g, 0.0967 mmol) in 50 mL of CH_3CN at room temperature. The highly-insoluble green product which formed within several minutes was washed with ether and vacuum-dried. Yield: 84 mg. Elemental analysis is not consistent with the expected formula, $[\{Cr(tmpa)(NCS)\}_2(O)PdCl_2](ClO_4)_2$. Anal. Calcd for $[\{Cr(tmpa)(NCS)\}_2(O)PdCl_2](ClO_4)_2$: C, 38.26; H, 3.04; N, 11.74. Found: C, 43.13; H, 3.43; N, 15.17. IR: ν_{as}(CrOCr) = 862, 846, 832 cm^{-1}; ν(C≡N) = 2053 s, 2106 m cm^{-1}. Unlike $[Cr(tmpa)(NCS)]_2O(ClO_4)_2 \cdot H_2O$ and all other (tmpa)Cr^{III} monomers and dimers reported to date, the $PdCl_2$ adduct lacks a strong pyridyl in-plane ring deformation band[13] near 623 cm^{-1}. The $PdCl_2$ complex could not be dissolved without decomposition, preventing its further characterization.

In an attempt to prepare $[Cr(tmpa)(NCSAg)]_2O(ClO_4)_4$, stoichiometric quantities of $AgNO_3$ and $[Cr(tmpa)(NCS)]_2O(ClO_4)_2 \cdot H_2O$ were allowed to react in aqueous solution. A precipitate of AgNCS formed, indicating the partial extraction of NCS^- from the chromium coordination sphere. Only unreacted $[Cr(tmpa)(NCS)]_2O(ClO_4)_2 \cdot H_2O$ was recovered upon subsequent addition of $LiClO_4$ to the reaction mixture.

Results and Discussion

$[Cr(tmpa)(NCSe)]_2O^{2+}$ was prepared from $[Cr(tmpa)(OH)]_2^{4+}$ in excellent yield by the nucleophilic displacement method reported for related pseudohalide ligands.[3] CrOCr and CN stretching frequencies are essentially identical to those of the thiocyanate analog, and electronic transitions at 357 and 416 nm correspond closely in both energy and intensity to the e_g–e_u* (355 nm, $\epsilon = 1.41 \times 10^4$ M^{-1} cm^{-1}) and b_{2g}–e_u* (417 nm, $\epsilon = 2.74 \times 10^3$ M^{-1} cm^{-1}) bands of $[Cr(tmpa)(NCS)]_2O^{2+}$.[7] Unlike the thiocyanate complex, however, $[Cr(tmpa)(NCSe)]_2O^{2+}$ exhibits an *irreversible* oxidative cyclic voltammogram (Figure 1) with anodic peak potentials of 1.15 and 1.74 V and a shoulder near 1.42 V vs NHE. No cathodic complement to the 1.15 V anodic peak could be resolved even when the sweep window was narrowed and the sweep rate was increased to 300 mV/s. In this respect, the voltammogram of $[Cr(tmpa)(NCSe)]_2O^{2+}$ closely resembles those of $[Cr(bpy)_2(NCS)]_2O^{2+}$ and $[Cr(phen)_2(NCS)]_2O^{2+}$ under the same conditions.[8] Considering that free $NCSe^-$ is a stronger reducing agent[9] than NCS^-, NCO^-, CN^-, N_3^-, and Cl^-, this

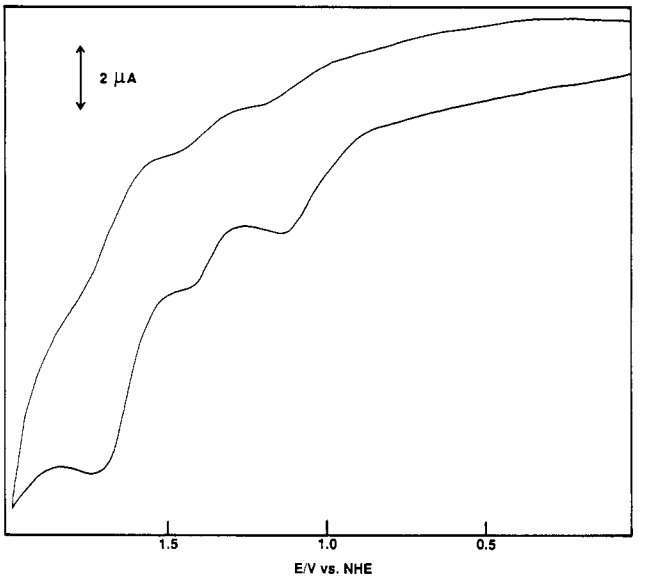

Figure 1. Cyclic voltammogram of $[Cr(tmpa)(NCSe)]_2O^{2+}$ in CH_3CN solution; Pt button working electrode, 25.0 °C, I = 0.1 M (TBAP), 50 mV/s sweep rate.

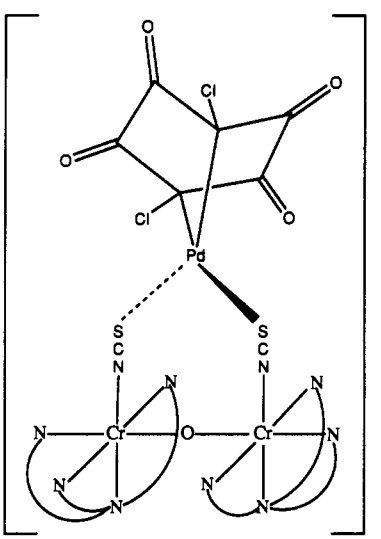

Figure 2. Proposed structure of $[\{Cr(tmpa)(NCS)\}_2(O)Pd(CA)]^{2+}$.

irreversibility most logically follows from intracomplex oxidation of ligated $NCSe^-$ by a Cr(III,IV) species generated in the wave at E_{pa} = 1.15 or 1.42 V. $[Cr(tmpa)(NCSe)]_2OH^{3+}$ (pK_a = 1.48) is more acidic than $[Cr(tmpa)(NCS)]_2OH^{3+}$ by a factor of 3.7, and $[Cr(tmpa)(NCSe)]_2O(ClO_4)_2$ is diamagnetic over the entire 4–300 K temperature range.

$[Pd(CA)(CH_3CN)_2]$ forms adducts with $[Cr(tmpa)(NCS)_2]^+$ and $[Cr(tmpa)(NCS)]_2O^{2+}$ in which the Pd(II) center is chelated by the pair of thiocyanate ligands from the chromium complex, $[Cr(tmpa)(NCS)_2Pd(CA)]^+$ and $[\{Cr(tmpa)(NCS)\}_2(O)Pd(CA)]^{2+}$. The proposed structure of the latter adduct is illustrated in Figure 2. The well-documented[12,14] carbon-bonded chloranilate ligand is characterized by (1) several strong C=O vibrations in the 1620–1720-cm^{-1} interval but no 1500–1550-cm^{-1} C—O mode; (2) a relatively high C—Cl stretching frequency (>855 cm^{-1}); and (3) a carbon-to-palladium(II) LMCT band near 300 nm but no π–π* bands in the vicinity of 340 and 540 nm characteristic of chloranilate in its *p*-quinonoid resonance form.[15] Both Pd(CA) adducts described here satisfy these IR and UV–vis criteria for C-bonded chloranilate. By comparison with $[Cr(tmpa)$-

(13) Clark, R. J. H.; Williams, C. S. *Inorg. Chem.* **1965**, *4*, 350.

(14) Jeong, W.-Y.; Holwerda, R. A. *J. Organomet. Chem.* **1989**, *372*, 453.
(15) Jeong, W.-Y.; Holwerda, R. A. *Inorg. Chem.* **1989**, *28*, 2674.

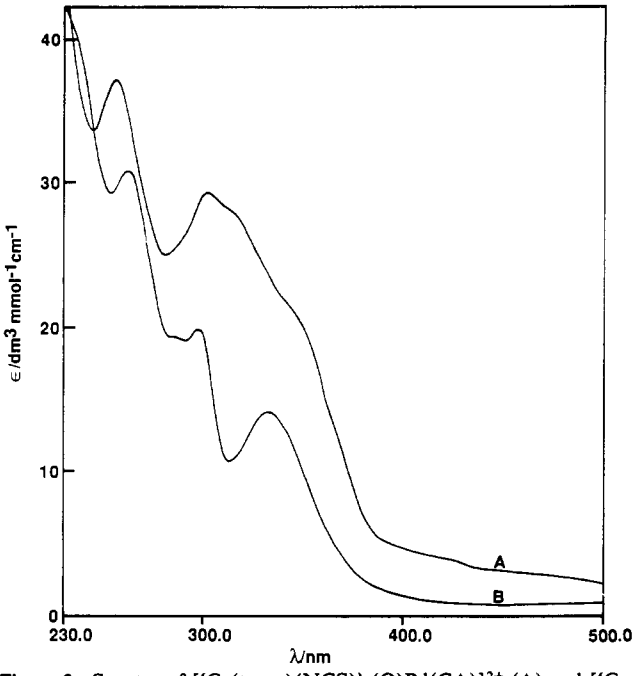

Figure 3. Spectra of $[\{Cr(tmpa)(NCS)\}_2(O)Pd(CA)]^{2+}$ (A) and $[\{Cr(tmpa)(NCS)\}_2(OH)Pd(CA)]^{3+}$ (B) in CH_3CN solution.

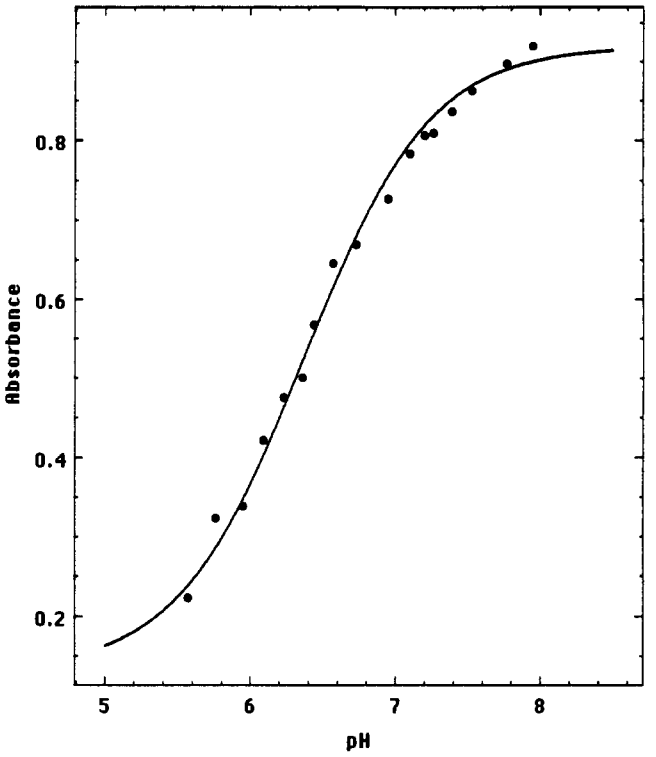

Figure 4. Spectrophotometric titration of $[Cr(tmpa)(O)(F)Cr(tmpa)]^{3+}$ at 331 nm; 25.0 °C, I = 0.1 M ($NaNO_3$), 1 cm path length, dimer concentration = 0.237 mM. Solid curve was calculated from nonlinear least-squares best fit parameters.

$(NCS)_2]^+$,[10] 263-, 299-, and 342-nm bands of $[Cr(tmpa)(NCS)_2Pd(CA)]^+$ are assigned to tmpa pyridyl $\pi-\pi^*$, chloranilate C-to-Pd(II), and NCS^--to-Cr(III) charge transfer transitions, respectively. These features agree well with the spectrum of $[\{Cr(tmpa)(NCS)\}_2(OH)Pd(CA)]^{3+}$ (Figure 3), generated by protonation of the oxo-bridged analog (λ_{max}, nm (ϵ, M^{-1} cm^{-1}): 264 (3.1×10^4), 299 (2.0×10^4), 334 (1.4×10^4)). The finding of carbon-bonded chloranilate in the $[Pd(CA)(SCN)_2]^{2-}$ coordination unit is not surprising, considering that $[Pd(CA)(CH_3CN)_2]$ and a thiocyanate-bridged palladium(II) dimer, $[Pd(CA)(\mu\text{-}NCS)]_2^{2-}$, favor this ligation mode over *o*- and *p*-quinone linkage isomers.[14]

Conversion of N-bonded thiocyanate to a bridging NCS^- ligand usually increases the CN stretching energy to >2100 cm^{-1};[9,16] for $K_2[Pd(CA)(\mu\text{-}NCS)]_2$,[14] ν(CN) = 2160 cm^{-1}. This bridging criterion is inconclusive for the complexes presently under consideration, however, as small shifts in ν(CN) from 2020 to 2035 cm^{-1} and from 2053 to 2049 cm^{-1} pertain upon the formation of Pd(CA) adducts with $[Cr(tmpa)(NCS)_2]^+$ and $[Cr(tmpa)(NCS)]_2O^{2+}$, respectively. Nevertheless, the elemental analysis data are consistent with the presence of six-coordinate Pd(II) centers in both $[\{Cr(tmpa)(NCS)\}_2(O)Pd(CA)](ClO_4)_2\cdot 2CH_3CN$ and $[Cr(tmpa)(NCS)_2Pd(CA)](ClO_4)\cdot 2CH_3CN$, composed of bidentate CA^{2-}, two S-bonded NCS^-, and two CH_3CN ligands. A difference spectrum between $[\{Cr(tmpa)(NCS)\}_2(O)Pd(CA)]^{2+}$ and $[\{Cr(tmpa)(NCS)\}_2(OH)Pd(CA)]^{3+}$ reveals peaks at 256 ($\Delta\epsilon = 9.4 \times 10^3$ M^{-1} cm^{-1}), 313 ($\Delta\epsilon = 1.8 \times 10^4$ M^{-1} cm^{-1}) and 355 nm ($\Delta\epsilon = 1.1 \times 10^3$ M^{-1} cm^{-1}). The close correspondence between e_g–e_u^* electronic transition and ν_{as}(CrOCr) vibrational energies of $[Cr(tmpa)(NCS)]_2O^{2+}$ and $[\{Cr(tmpa)(NCS)\}_2(O)Pd(CA)]^{2+}$ shows that the CrOCr chromophore is essentially unperturbed by adduct formation with Pd(CA). The intensity of the $[Cr(tmpa)(NCS)]_2O^{2+}$ NCS^--to-Cr(III) LMCT band at 313 nm ($\epsilon = 1.1 \times 10^4$ M^{-1} cm^{-1})[7] is smaller than $\Delta\epsilon_{313}$ of the Pd(CA) adduct, as expected from the transition dipole moment increase associated with rotation of both NCS^- ligands to one side of the CrOCr bond axis.

The oxidative cyclic voltammogram of $[\{Cr(tmpa)(NCS)\}_2(O)Pd(CA)]^{2+}$ exhibits no peaks from 0 V to the CH_3CN solvent cutoff. An anodic shoulder with a weak cathodic counterpart was observed near +1.2 V vs NHE, however, in the same vicinity as the one-electron oxidation wave of the parent chromium dimer. Evidently, blocking of the thiocyanate S atoms markedly slows the heterogeneous electron transfer rate. In similar fashion to the selenocyanate derivative, the acidity of $[\{Cr(tmpa)(NCS)\}_2(OH)Pd(CA)]^{3+}$ ($pK_a = 1.15$) exceeds that of $[Cr(tmpa)(NCS)]_2OH^{3+}$ by a factor of 7.9 and $[\{Cr(tmpa)(NCS)\}_2(O)Pd(CA)](ClO_4)_2\cdot 2CH_3CN$ is diamagnetic between 4 and 300 K. For comparison purposes, the magnetic susceptibility of $[Cr(bpy)_2(NCS)]_2OH(ClO_4)_3\cdot 2H_2O$ was examined over the same temperature interval and a spectrophotometric titration of $[(tmpa)Cr(O)(F)Cr(tmpa)]^{3+}$ was performed (Figure 4). As compared with $[Cr(tmpa)(OH)]_2^{4+}$, the isoelectronic fluoro, hydroxo-bridged dimer is more acidic by a factor of 18. Table I presents a comparison among the acid–base, magnetic, and electrochemical characteristics of oxo- and hydroxo-bridged Cr(III) dimers with aromatic amine or diimine ligands.

The disposition of tetradentate tmpa ligands with regard to the oxo bridge of dinuclear complexes may be either symmetric (both apical N atoms cis to μ-O^{2-}) or unsymmetric (one apical N atom cis and the other trans to μ-O^{2-}).[7,10,17-19] Que and coworkers recently described an NMR approach that can be used to distinguish between these configurations.[18,19] Unsymmetric chelation gives rise to three peaks with relative intensities 2:1:3 in the 6–8 ppm interval for tmpa pyridyl protons para to the N donor atom. In contrast, symmetric dimers are characterized by a two-peak pattern with intensity ratio 2:4 in the same chemical shift range. Thus, two pyridyl N atoms are trans to the oxo bridge while four are trans to other pyridyl N atoms in the

(16) Palaniappan, V.; Sathaiah, S.; Bist, H. D.; Agarwala, U. C. *J. Am. Chem. Soc.* **1988**, *110*, 6403.

(17) Gafford, B. G.; Marsh, R. E.; Schaefer, W. P.; Zhang, J. H.; O'Connor, C. J.; Holwerda, R. A. *Inorg. Chem.* **1990**, *29*, 4652.

(18) Norman, R. E.; Yan, S.; Que, L., Jr.; Backes, G.; Ling, J.; Sanders-Loehr, J.; Zhang, J. H.; O'Connor, C. J. *J. Am. Chem. Soc.* **1990**, *112*, 1554.

(19) Norman, R. E.; Holz, R. C.; Menage, S.; O'Connor, C. J.; Zhang, J. H.; Que, L., Jr. *Inorg. Chem.* **1990**, *29*, 4629.

Table I. Comparison of Physical Properties for Oxo- and Hydroxo-Bridged Cr(III) Dimers

complex (code)	pK_a[a]	J, cm^{-1}	$E_{1/2}$, V vs NHE[b]	ref
$[Cr(bpy)_2(NCS)]_2O^{2+}$	<0	−247	1.29 (E_{pa})	8
$[Cr(bpy)_2(NCS)]_2OH^{3+}$		−11.0[c]		this work
$[Cr(phen)_2(NCS)]_2O^{2+}$	<0	−271	1.29 (E_{pa})	8
$[Cr(tmpa)(NCS)]_2O^{2+}$ (1)	2.05	−255	1.17	3,7
$[\{Cr(tmpa)(NCS)\}_2(O)Pd(CA)]^{2+}$	1.15(0.09)	diamagnetic[d]		this work
$[Cr(tmpa)(NCO)]_2O^{2+}$ (2)	4.09		1.02	3
$[Cr(tmpa)(NCSe)]_2O^{2+}$	1.48(0.06)	diamagnetic[d]	1.15 (E_{pa})	this work
$[Cr(tmpa)(N_3)]_2O^{2+}$ (3)	4.25		0.96	3
$[Cr(tmpa)(CN)]_2O^{2+}$ (4)	0.64	−290	1.17	3
$[Cr(tmpa)Cl]_2O^{2+}$ (5)	4.01[e]		1.03	3
$[Cr(tmpa)(OH)(O)Cr(tmpa)]^{3+}$ (6)	7.50	−68.5	0.62	3,10,11
$[Cr(tmpa)(OH)]_2^{4+}$		−15.7		3
$[Cr(tmpa)(O)(F)Cr(tmpa)]^{3+}$ (7)	6.25(0.04)		0.74	11, this work
$[(tmpa)Cr(O)(HCO_2)(tmpa)]^{3+}$ (8)	1.69	−93.0	1.21	17
$[(tmpa)Cr(O)(CH_3CO_2)Cr(tmpa)]^{3+}$ (9)	2.20	−50.3	1.17	17
$[(tmpa)Cr(O)(C_6H_5CO_2)Cr(tmpa)]^{3+}$ (10)	1.88	−75.4	1.22	17

[a] pK_a based on the ionization constant of conjugate Cr(OH)Cr acid; 25.0 °C, I = 0.1 M ($NaNO_3$). For spectrophotometric titrations of $[\{Cr(tmpa)(NCS)\}_2(O)Pd(CA)]^{2+}$, $[Cr(tmpa)(NCSe)]_2O^{2+}$, and $[Cr(tmpa)(O)(F)Cr(tmpa)]^{3+}$, wavelengths and pH ranges used were 313 (pH 1.12–2.82), 357 (pH 1.12–3.81), and 331 (pH 2.96–10.37) nm, respectively. Standard deviations are shown in parentheses. [b] Cr(III,IV/III,III) half-wave reduction potential, measured at 25.0 °C, I = 0.1 M (TBAP) in CH_3CN. [c] Other non-linear least-squares best fit parameters for $[Cr(bpy)_2(NCS)]_2OH(ClO_4)_3 \cdot 2H_2O$ are g = 2.012, TIP = 1.05 × 10^{-3} emu/mol, % impurity with Curie–Weiss behavior = 1.5%. [d] $-2J \geq 1000$ cm^{-1}. [e] pK_a estimated from a linear pK_a vs $10Dq$ correlation for $[Cr(tmpa)L]_2O^{2+}$ dimers.[3]

Table II. Comparison of ^{1}H Chemical Shifts for $[Cr(tmpa)L]_2O^{2+}$ Dimers[a]

	δ (number of protons)			
complex	CH_2	py *p*-H	py *m*-H	py *o*-H
$(tmpaH_3)^{3+}$	4.26 (6)	8.51 (3)	7.95 (3)	8.70 (3)
			8.04 (3)	
$[Cr(tmpa)(NCS)]_2O^{2+}$	6.49 (12)	7.26 (4)	5.47 (4)	7.76 (2)
		7.44 (2)	6.13 (8)	8.83 (4)
$[\{Cr(tmpa)(NCS)\}_2(O)Pd(CA)]^{2+}$	6.49 (12)	7.24 (4)	5.44 (4)	7.77 (2)
		7.41 (2)	6.13 (8)	8.85 (4)
$[Cr(tmpa)(NCO)]_2O^{2+}$	6.49 (12)	7.19 (4)	5.38 (4)	7.97 (2)
		7.26 (2)	5.97 (8)	8.94 (4)
$[Cr(tmpa)(NCSe)]_2O^{2+}$	6.50 (12)	7.29 (4)	5.47 (4)	7.71 (2)
		7.49 (2)	6.16 (8)	8.83 (4)
$[Cr(tmpa)(N_3)]_2O^{2+}$	6.79 (12)	7.19 (4)	5.32 (4)	7.93 (2)
		7.32 (2)	5.98 (8)	8.88 (4)
$[Cr(tmpa)(CN)]_2O^{2+}$	6.97 (12)	7.35 (8)[b]	5.78 (4)	8.20 (4)
			6.42 (8)	
$[Cr(tmpa)Cl]_2O^{2+}$	*c*	7.19 (6)	5.56 (4)	7.97 (2)
			6.04 (8)	8.93 (4)

[a] Measured in CD_3CN at ambient temperature; chemical shifts referenced to TMS. [b] Overlapping tmpa para H and ortho H resonances. [c] Broad resonance, peak position not clearly resolved.

symmetric ligation mode. Symmetric chelation is proven for $[Cr(tmpa)(NCS)]_2O^{2+}$ by X-ray crystallography,[7] but has not yet been established for other dimers in this class. In order to resolve this issue, ^{1}H NMR spectra have been acquired for all $[Cr(tmpa)L]_2O^{2+}$ complexes prepared to date (Table II). Two pyridyl para H resonances with the predicted 2:4 intensity ratio are in fact resolved in the 7.0–7.5 ppm range for all $[Cr(tmpa)L]_2O^{2+}$ complexes except those with L = CN^- and Cl^-, where a single resonance is observed. The assignment of symmetric tmpa ligation throughout the entire series is further supported by pyridyl ortho H and meta H resonances, which occur in pairs with intensity ratios of 2:4 and 4:8, respectively. Although the NMR results are also consistent with the geometric isomer in which both apical nitrogen atoms are trans to the μ-O^{2-} group, such a structure is contrary to solid-state findings for $[Cr(tmpa)(NCS)]_2O^{2+}$,[7] $[Fe(tmpa)Cl]_2O^{2+}$,[19] and $[V(tmpa)(O)]_2O^{2+}$.[20] Chemical shift similarities among the NMR spectra for dimers with NCS^-, $NCSe^-$, and $NCS\{Pd(CA)/2\}^-$ substituents clearly indicate parallelisms in both their geometric and electronic structures.

Factors which influence the CrOCr π-bonding energy in $[CrN_4L]_2O^{2+}$ complexes include the Cr–O–Cr bond angle, the π-accepting strength of aromatic polyamine or diimine ligands (N_4) and the π-donating ability of L^-. In our work, both unsupported[3,7,8] and doubly-bridged μ-O^{2-} chromium(III) dimers with hydroxo,[10] fluoro,[11] or carboxylato[17] supporting groups have been investigated. Figure 5 displays a remarkably good linear correlation of Cr(III,IV/III,III) half-wave reduction potential vs pK_a of Cr(μ-OH)Cr, including *all* (tmpa)CrOCr(tmpa) dimers for which both $E_{1/2}$ and pK_a values are available (Table I). Thus, with the exception of $[Cr(tmpa)(CN)]_2O^{2+}$, both singly- and doubly-bridged dimers follow the relationship $E_{1/2} = 1.40 - 0.10(pK_a)$ V (correlation coefficient = 0.994) over a range spanning nearly 6 orders of magnitude in bridging oxo group basicity. This correlation demonstrates that the b_{2g} HOMO energy increases in the order μ-$C_6H_5CO_2^- \approx \mu$-$HCO_2^- < \mu$-$CH_3CO_2^- \approx NCS^- < NCO^- \approx Cl^- < N_3^- \ll \mu$-$F^- < \mu$-$OH^-$, closely paralleling enhancements in π-donor capabilities of both bridging and non-bridging substituents. Looked at from another perspective, Figure 5 represents a linear free energy relationship between one-electron oxidation and protonation reactions of oxo-bridged dimers. Fenske–Hall calculations on linear L_5MOML_5 complexes predict the molecular orbital energy ordering $e_g < b_{2g} < b_{1u}$ when L is a π-donor, in contrast to the $b_{2g} < b_{1u} < e_g$ ranking which pertains in the presence of π-acceptor ligands.[21] Of particular importance is the predicted high sensitivity of the b_{2g} level to destabilization by π-donor ligands, owing to negative overlap between eight of

(20) Toftlund, H.; Larsen, S.; Murray, K. S. *Inorg. Chem.* **1991**, *30*, 3964.

(21) Lin, Z.; Hall, M. B. *Inorg. Chem.* **1991**, *30*, 3817.

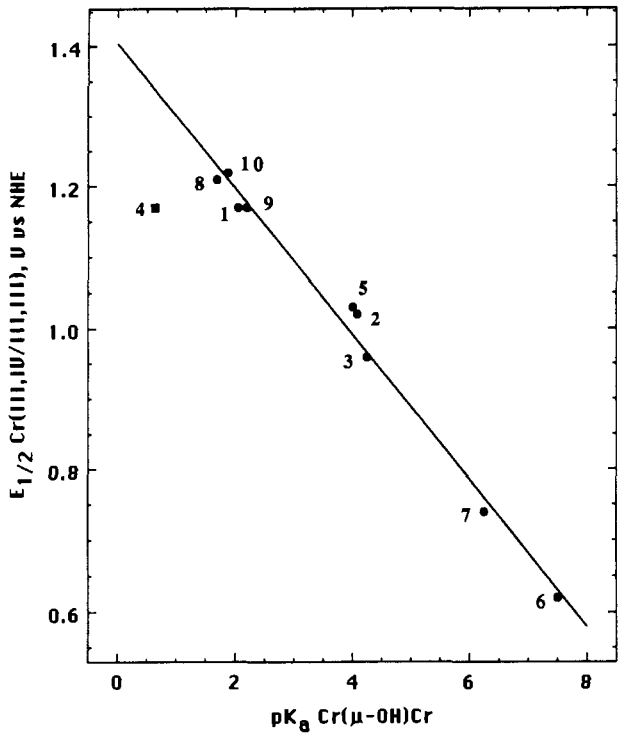

Figure 5. Correlation of Cr(III,IV/III,III) half-wave reduction potentials with bridging oxo group basicity for singly- and doubly-bridged CrOCr dimers. $E_{1/2}$, pK_a values and complex code numbers taken from Table I. The point for L = CN^- (**4**, ■) was excluded from the least-squares fit shown by the solid line.

ten L^- π-donor orbitals and two metal d_{xy} orbitals per dimeric unit.[21] The failure of CN^- to fall on the $E_{1/2}$ vs pK_a correlation line is not surprising, considering that cyanide, a strong field ligand, is the only L^- group presently under consideration whose π-donor strength is vastly overshadowed by its π-acceptor capability.

Conjugation of μ-O^{2-} group lone pairs with Cr($d\pi$) orbitals restricts their susceptibility to protonation. Therefore, to a reasonable level of approximation, bridging oxygen atom basicity may be treated as a measure of π-bonding strength in CrOCr dimers.[3,7,8,10,17] Such a treatment presumes that steric factors and solvation free energy differences between μ-O^{2-} and μ-OH^- species remain essentially constant throughout the series under consideration. The trend towards larger pK_a of Cr(μ-OH)Cr conjugate acids with increasing π Lewis basicity of L^- illustrated in Figure 5 shows that CrOCr π-bonding strength is sensitive to the competition between μ-O^{2-} and μ-X^- or L^- substituents for donation to the metal. Thus, the weakest π-donor L^- groups enable the Cr–bridging oxo overlap to be maximized. This point is underscored by the finding of negative shifts in pK_a upon the substitution of NCS^- by $NCSe^-$ or NCS{Pd(CA)/2}$^-$ in $[Cr(tmpa)L]_2O^{2+}$ dimers. It should also be noted that Cr(μ-OH)Cr acidity is enhanced by strong field ligands, as is shown by the L^- = CN^- and N_4 = $(bpy)_2$ or $(phen)_2$ results. Such an effect may be understood in terms of the decreasing energy difference between overlapping oxo 2p donor and Cr 3d acceptor orbitals.[3]

Antiferromagnetic coupling in hydroxo- and oxo-bridged chromium(III) dimers is governed by the Cr–O–Cr bond angle, hybridization of the bridging oxygen atom, Cr···Cr distance, Cr–bridging oxygen bond length, and crystal packing effects.[22,23] Unlike multiply-bridged FeOFe species,[24] Cr(III) dimer magnetic susceptibilities do not vary simply with the shortest superexchange pathway.[22] We report here the first two examples of oxo-bridged chromium(III) complexes which are diamagnetic over the entire 4–300 K temperature interval. Comparatively large singlet–triplet gaps ($-2J \geq 1000$ cm^{-1}) in the (selenocyanato)- and (chloranilato)palladium(II) derivatives correspond to b_{2g}(HOMO)–b_{1u}(LUMO) separations (Δ) enhanced by the weaker π-donor abilities of $NCSe^-$ and NCS{Pd(CA)/2}$^-$ relative to NCS^- ($-2J = 510$ cm^{-1}). Thus, Δ is thought to increase with decreasing configuration interaction between the metal-centered HOMO ($3d_{xy}(1) + 3d_{xy}(2)$) and the lower-lying pseudohalide ligand b_{2g} symmetry orbital. On protonation of an unsupported oxo bridge, the antiferromagnetic coupling between Cr(III) centers falls off dramatically. Thus, the coupling constant reported here for $[Cr(bpy)_2(NCS)]_2OH^{3+}$ amounts to only 4.5% of that for $[Cr(bpy)_2(NCS)]_2O^{2+}$, consistent with findings for $[Cr(NH_3)_5]_2OH^{3+}$ ($J = -15.8$ cm^{-1}) and $[Cr(NH_3)_5]_2O^{2+}$ ($J = -225$ cm^{-1}); J(μ-OH^-) = 7.0% of J(μ-O^{2-}).[25]

In order to further test the generality of a linear free-energy relationship between one-electron oxidation and protonation reactions of both singly and doubly-bridged Cr(III)–O–Cr(III) dimers, we are presently exploring the reactivities of $[(tmpa)Cr(\mu\text{-}O)(\mu\text{-}X)Cr(tmpa)]^{3+}$ species in which the supporting bridge offers N, S, or O donor atoms. The possibility of bond-making between μ-O^{2-} and μ-X^- groups subsequent to one- or two-electron oxidation of the metal centers is of particular interest.

Acknowledgment. R.A.H. thanks the Welch Foundation (Grant D-735) for support of this research and Drs. B. G. Gafford and W.-Y. Jeong for suggesting the synthesis of (chloranilato)-palladium(II) adducts with (thiocyanato)chromium(III) complexes.

(22) Spiccia, L.; Fallon, G. D.; Markiewicz, A.; Murray, K. S.; Riesen, H. *Inorg. Chem.* **1992**, *31*, 1066.
(23) Glerup, J.; Hodgson, D. J.; Pedersen, E. *Acta Chem. Scand.* **1983**, *A37*, 161.
(24) Gorun, S. M.; Lippard, S. J. *Inorg. Chem.* **1991**, *30*, 1625.
(25) Pedersen, E. *Acta Chem. Scand.* **1972**, *26*, 333.